ELSEVIER

Biochimica et Biophysica Acta 1457 (2000) 106–117

BIOCHIMICA ET BIOPHYSICA ACTA
BBA

www.elsevier.com/locate/bba

Interaction of photosynthetic pigments with various organic solvents 2 Application of magnetic circular dichroism to bacteriochlorophyll *a* and light-harvesting complex 1

Mitsuo Umetsu, Zheng-Yu Wang, Kenzi Yoza, Masayuki Kobayashi, Tsunenori Nozawa *

Department of Biomolecular Engineering, Graduate School of Engineering, and Center for Interdisciplinary Research, Tohoku University, Aobayama 07, Aoba-ku, Sendai 980-8579, Japan

Received 13 August 1999; received in revised form 4 January 2000; accepted 19 January 2000

Abstract

Magnetic circular dichroism (MCD) and absorption spectra of metal bacteriochlorin complexes have been measured on bacteriochlorophyll (BChl) *a* in various solvents and different forms of light-harvesting complexes 1 (LH1 complexes). In hydrophilic organic solvents, the MCD intensity of the $Q_y(0–0)$ transition of BChl *a* was sensitive to the wavelength of absorption maximum of $Q_x(0–0)$, and the ratio of MCD $Q_y(0–0)$ intensity to the dipole strength (*B*/*D*) was inversely proportional to the difference in energy between the $Q_x(0–0)$ and $Q_y(0–0)$. The similar correlation has been observed in metal chlorin derivatives as previously reported. The correlation depends on the coordination number of the Mg atom in BChl *a* and the molecules ligating to it. In a hydrophobic solvent such as carbon tetrachloride (CCl_4), however, the correlation did not hold because of the existence of aggregates. Hence, the correlation between the values of *B*/*D* and the energy difference can be used to estimate the type and number of the molecules ligated to the Mg atom and to disclose the existence of aggregated pigments. We further apply the correlation to the LH 1 complex treated with *n*-octyl β-D-glucopyranoside.

Keywords: Magnetic circular dichroism; Bacteriochlorophyll *a*; Coordination state; Light-harvesting complex 1; *n*-Octyl-β-D-glucopyranoside (β-OG) treatment

1. Introduction

Chlorophyll (Chl) *a* and bacteriochlorophyll (BChl) *a* perform important roles in the light reaction in photosynthesis [1,2]. The pigments are functioning in the light-capture and energy-transducing systems and usually are held in proteins, such as, antenna complexes of purple bacteria and reaction centers in green plants and bacteria. It is crucial to understand the nature of the pigments in order to elucidate the mechanism of photosynthesis, and consequently, Chl *a* and BChl *a* molecules have been profoundly investigated with various spectroscopic methods: absorption [3–9], infrared and resonance Raman [10–17], X-ray diffraction [1], and nuclear magnetic resonance [18–24]. (B)Chl *a* contains a Mg atom in the center of macrocycle, which is coordinated by four pyrrole nitrogens. However, the Mg

* Corresponding address. Fax: +81-22-217-7279; E-mail: nozawa@biophys.che.tohoku.ac.jp

0005-2728/00/$ – see front matter
PII: S0005-2728(00)00070-0

atom is not satisfied with the four-coordination and one or two axial ligands further coordinate to the Mg atom. The coordination state of the Mg atom is one of the most important subjects in structural studies of light harvesting (LH) complexes and reaction centers.

The absorption spectrum of (B)Chl *a* is characterized by two *x*- and *y*-polarized bands in the near-ultra violet region (B_x, B_y) and in the visible region (Q_x, Q_y). The Q_x band of BChl *a* is known to shift by changing of the coordination state and the shift of the Q_x band is used to distinguish between the five- and six-coordinated species [5,9,15,25]. However for Chl *a*, determination of the coordination species from the only absorption spectra is difficult since the Q_x band is weak and hardly discernible. Whereas, the infrared and resonance Raman spectra can be used to analyze not only the coordination state of metal bacteriochlorin but also those of metal chlorin and porphyrin derivatives [12,13,15,16]. Three bands in 1620–1510 cm^{-1}, which are assigned to C=C stretching in macrocycle, are downshifted when the coordination state changes from five- to six-coordinated species. Recently, the analysis is applied to LH complexes [26–29] and reaction centers [30,31].

The magnetic circular dichroism (MCD) spectra of porphyrin [32–34], chlorin and bacteriochlorin [35–42] derivatives have been extensively measured because MCD is sensitively dependent on the degeneracy of the lowest unoccupied molecular orbitals (LUMOs) and the highest occupied molecular orbitals (HOMOs). Especially, the MCD of hemes with porphyrin backbones had been studied in order to elucidate the function of the central metal and electron-acceptance/donation, such as, oxygen binding of a hemoglobin and electron transfer of cytochromes [33,43]. The MCD properties are dramatically varied with the change of the electronic states of the hemes by ligation in the central metal or by electron transfer. In the case of chlorin and bacteriochlorin derivatives, the MCD of the pigments in vitro had been observed and Michl [44,45] suggested a rule for prediction of MCD signs of B_x, B_y, Q_x and Q_y on the basis of the two energy differences between the next HOMO and HOMO, and the LUMO and next LUMO. Keegan et al. [37,38] reported the results supporting the prediction from MCD measurements of various artificial pigments. Whereas in vivo, application of MCD has not been systematically applied in comparison with porphyrin derivatives. We have recently found that the MCD spectra of photosynthetic pigments with chlorin backbones in the visible region are sensitive to the coordination state of the central metal, and the ratio of Q_y intensity of MCD spectra to the dipole strength (B/D) is correlated with the energy difference between the Q_x and Q_y transitions [42]. It will be possible to determine the coordination number and the relative bonding strength of ligands.

In this study, we are concerned with BChl *a* as one of the predominant metal bacteriochlorin derivatives in photosynthetic bacteria and have analyzed the correlation between the values of B/D and the difference in energy of Q_x and Q_y. Comparison of the Mg complexes between chlorin and bacteriochlorin provides important information on the influence of the structural difference in the macrocycle on the mixing between dipole moments. We also measured the absorption and MCD spectra of aggregated BChl *a* in carbon tetrachloride (CCl_4) and a LH1 complex, and then compared the correlations with those of monomeric BChl *a* in hydrophilic organic solvents. The LH1 complex used in this study is composed of oligomers of a subunit structure containing carotenoids, two BChl molecules, and two small polypeptides (α, β peptide), and in the complex, the Mg atoms of two BCh *a* are ligated by each histidyl residue in the α, β peptides. The Q_y transition of the complex is known to blue-shift from 877 to 820 nm, and finally to 777 nm, with increase of the concentration of *n*-octyl-β-D-glucopyranoside (β-OG) [46,47]. This blue-shift is probably due to dissociation of the LH1 complex absorbing at 877 nm (B877 form) to smaller unit forms (B820 and B777 forms, respectively). In order to elucidate the interaction with BChl *a* and histidyl residue, we compared the values of B/D and the energy difference between the Q_x and Q_y for the BChl *a* ligated by imidazole and the B777 complex.

2. Materials and methods

2.1. Materials

BChl *a* was extracted from *Rhodospirillum rubrum*

with a mixture of methanol and acetone at a ratio of 1:1 and purified with a reversed phase HPLC column as previously reported [48]. The purified LH1 complex was obtained from *R. rubrum* with the method reported previously and dissolved in 50 mM phosphate buffer with the treatment of 0.46% β-OG [49]. The organic solvents used were of spectroscopic grade and molecular sieves (3A) of Wako Pure Chemical Industries were used to remove trace water. Dichloromethane (CH_2Cl_2) and CCl_4 were treated with Na_2CO_3.

2.2. Instrument and spectroscopic methods

Absorption spectra were recorded on a Beckman DU-640 spectrophotometer with a 1 cm quartz cuvette. MCD spectra were measured from 900 to 400 nm on a Jasco J-720w spectropolarimeter with a 1 cm quartz cuvette. The conditions of MCD measurement were as follows: slit width: 60 μm, resolution: 0.5 nm, response: 1 s, scan speed: 20 nm/min and external magnetic field: 1.5 T.

BChl *a* was dissolved in various hydrophilic organic solvents (diethyl ether, acetone, THF, dioxane and pyridine), CH_2Cl_2 and CCl_4. Imidazole and indole were added in each of the CH_2Cl_2 solutions to the concentration of 3.3 M. The concentration of BChl *a* in all the solutions was 1.3×10^{-5} mol l^{-1} and the extinction coefficients were calculated on the basis of a value of 91.0×10^4 l $(mol\times cm)^{-1}$ in diethyl ether. The LH1 complex in phosphate buffer was treated with 0.46%, 0.75% and 4.0% β-OG, separately.

The deconvolutions of absorption and MCD spectra were performed using the non-linear curve fitting tool of a software GRAMS/32 V5.0 (Galactic), according to a method similar to that reported previously [42]; that is, (1) each pair of the absorption and MCD spectra was deconvoluted into the same number of the components which have the same band center and band width parameters; (2) a mixed Gaussian-Lorentzian function was used to fit each component; (3) the deconvolution continued until χ^2 (the sum of squares of the deviations normalized by the variance of count) attained less than three.

3. Results

3.1. Monomeric BChl a in hydrophilic organic solvents

Fig. 1 shows the absorption and MCD spectra of BChl *a* in mixed solution of diethyl ether and pyridine. The absorption spectrum observed in neat diethyl ether, showed Q_x(0–0) and Q_y(0–0) transitions at 574 nm and 770 nm, respectively. The Q_x(0–0) was red-shifted to 606 nm by titration of pyridine in the diethyl ether solution, while the Q_y(0–0) was only slightly shifted. The little shift of Q_y(0–0) was also observed in the MCD spectra, however, the MCD intensity of Q_y(0–0) was increased more than that of the absorption as pyridine was added in the diethyl ether solution. Considering that no aggregation occurs in the diethyl ether solution and the Mg atom of BChl *a* is known to be five-coordinated in diethyl ether and six-coordinated in pyridine [12,15], the spectral change is due to difference of the coordination state.

In order to understand the cause for the increase of the Q_y(0–0) MCD intensity quantitatively, the ab-

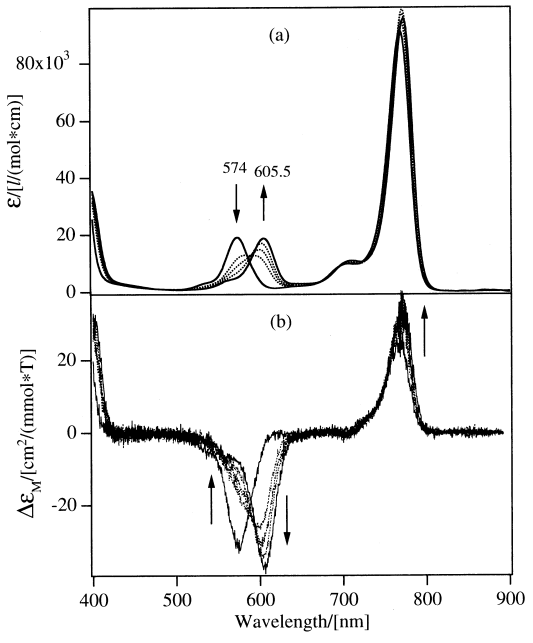

Fig. 1. Absorption (a) and MCD (b) spectra of BChl *a*/diethyl ether solution titrated by pyridine. The concentration of BChl *a* was calculated as 1.3×10^{-5} mol/l. The volumes of pyridine added into 3 ml diethyl ether were 0, 10, 20, 50 and 350 μl.

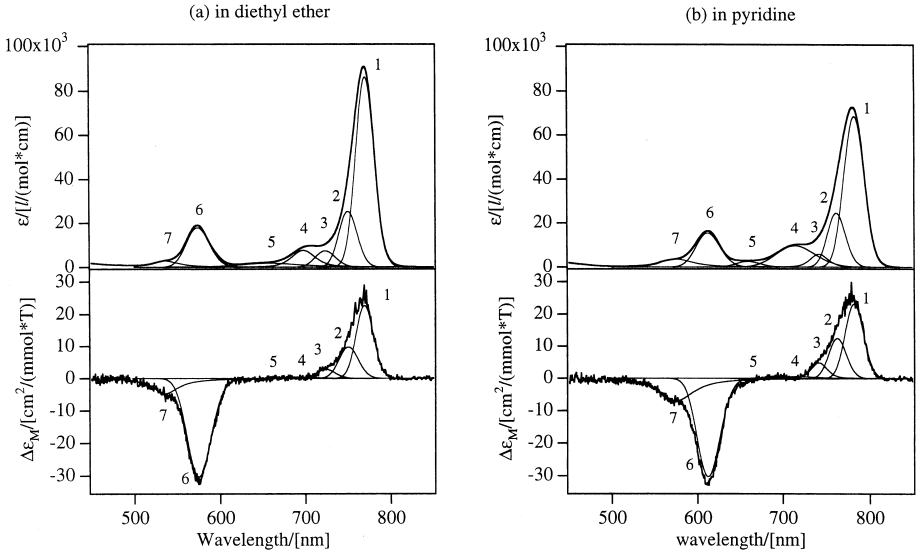

Fig. 2. Deconvolution of the absorption and MCD spectra of BChl *a* in diethyl ether (a), and in pyridine (b).

sorption and MCD spectra were measured on BChl *a* in various hydrophilic organic solvents followed by deconvoluting the spectra simultaneously. In the deconvolution, the same parameters were used to fit pairs of associated components in the absorption and MCD spectra, i.e., the same number of components, the same band centers and half-widths of maximum intensity. Fig. 2 shows the deconvolution results for BChl *a* in diethyl ether and in pyridine, and Table 1 summarized the fitting parameters. The bands 1 and 6 apparently correspond to the Q_y(0–0) and Q_x(0–0) transition, respectively. For both solvents, seven fitting components were required for a satisfactory fitting and the bands 4 and 5 were contributed only slightly on the MCD spectra. For other solvents (acetone, dioxane and THF), the spectra could also be deconvoluted with seven fitting components and the bands 4 and 5 were weak in the MCD activity, as well (data not shown). The MCD spectra of BChl *a* are dominated by the Faraday *B*-term, which arises from the mixing between electronic states and is inversely proportional to the difference in energy between these states. In pyridine, the bands 3, 6 and 7 were relatively closer to the band 1 (Q_y(0–0)) than those in diethyl ether (Table 1). Since the ratio of the MCD *B*-term to the absorption dipole strength (*B*/*D*) is often used for a quantitative argument of the MCD intensity, we tried to correlate the *B*/*D* values of Q_y(0–0) with the energy difference between the Q_y(0–0) and other bands in all the sol-

Table 1
Fitting parameters for BChl *a* in diethyl ether and pyridine (in parentheses)

Band	λ (nm)	ε (10^3 l (mol×cm)$^{-1}$)	$\Delta\varepsilon_M$ (cm^2/(mmol×T))	Δcm^{-1}[a] (cm^{-1})	B/D[b] (kβ/cm^{-1})
1	770.0 (782.0)	86.2 (68.4)	22.6 (23.1)		26.4 (33.4)
2	750.1 (761.7)	25.3 (24.6)	9.71 (12.44)	345 (340)	
3	723.5 (741.7)	7.41 (5.85)	2.79 (4.83)	835 (695)	
4	697.6 (713.9)	7.65 (9.62)	0.36 (0.56)	1348 (1219)	
5	656.9 (659.0)	1.78 (2.41)	−0.10 (−0.22)	2235 (2386)	
6	573.8 (612.2)	17.9 (15.4)	−30.4 (−30.3)	4441 (3546)	
7	535.6 (574.7)	2.80 (3.59)	−4.67 (−6.93)	5684 (4613)	

[a]The Δcm^{-1} is the difference of wavenumber between each band and the band 1.
[b]The MCD *B*-term was calculated from molar ellipticity $\Delta\varepsilon_M$ as [40]: $B = 9.836\times10^5\int_{band}\Delta\varepsilon_M(\upsilon)/\upsilon d\upsilon$, where υ is wavenumber. The absorption dipole strength was calculated from the extinction coefficient ε as [40]: $D = 9.1834\times10^{-3}\int_{band}\varepsilon(\upsilon)/\upsilon d\upsilon$.

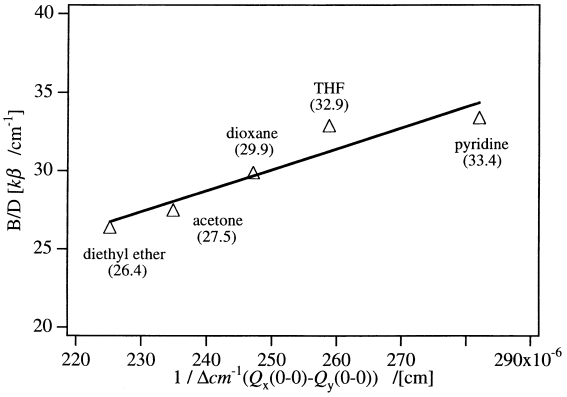

Fig. 3. Correlation between $B/D(Q_y(0–0))$ and $1/\Delta cm^{-1}(6-1)$ for BChl *a* in various solvents, where $\Delta cm^{-1}(6-1)$ represents the wavenumber difference between the bands 6 and 1. The solid line is the least squares line for BChl *a* in organic solvents. The *B*/*D* values of the $Q_y(0–0)$ are in parentheses.

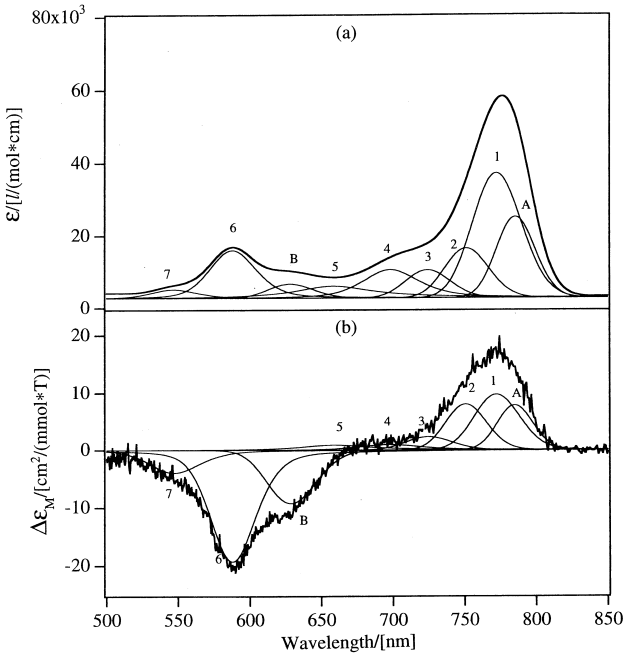

Fig. 4. Deconvolution of the absorption (a) and MCD (b) spectra of BChl *a* in imidazole-added CH_2Cl_2 solution. The concentrations of BChl *a* and imidazole were 1.3×10^{-5} mol/l and 3.3 mol/l, respectively.

vents. Good correlation was obtained only for the band 6 ($Q_x(0–0)$) (Fig. 3), whereas, no correlations for other bands (data not shown). Therefore, the energy difference between $Q_y(0–0)$ and $Q_x(0–0)$, which is caused by the change of the coordination state, made influences on the $Q_y(0–0)$ MCD intensity.

3.2. The ligation of imidazole and in vitro aggregates

For the purpose of analyzing interaction of BChl *a* with histidyl residues, we measured the absorption and MCD spectra of BChl *a* solutions containing imidazole. Fig. 4 shows the spectra and deconvolution results of BChl *a* in the imidazole-added CH_2Cl_2 solution. The high concentration of imdazole at 3.3 M was used to completely prevent aggregation of BChl *a*. Although the $Q_x(0–0)$ transition appeared at 579 nm in neat CH_2Cl_2, the $Q_x(0–0)$ was being red-shifted to 630 nm with a pseudoisosbestic point and the $Q_y(0–0)$ band was also red-shifted a little as the amount of imidazole was increasing (data not shown). Consequently, the $Q_x(0–0)$ bands appeared at 585 nm and 630 nm in the 3.3 M imidazole-added solution. This red-shift of the $Q_x(0–0)$ indicates the coordination by imidazole molecules. In order to deconvolute the spectra in the solution, one more component (the band B) was needed in the Q_x region besides the components used in hydrophilic solvents.

Table 2
Fitting parameters for BChl *a* in 3.3 M imidazole-added and 3.3 M indole-added (in parentheses) CH_2Cl_2 solutions

Band	λ (nm)	ε (10^3 l (mol×cm)$^{-1}$)	$\Delta\varepsilon_M$ (cm^2/(mmol×T))	*B*/*D* (kβ/cm^{-1})
A	785.7	22.5	7.82	38.7
1	772.4 (782.5)	34.4 (56.4)	9.71 (15.3)	30.1 (26.1)
2	751.2 (753.9)	13.7 (23.1)	8.02 (9.37)	
3	724.0 (718.9)	7.75 (11.2)	2.26 (3.63)	
4	698.1 (689.9)	7.84 (5.37)	0.97 (1.21)	
5	658.3 (653.7)	3.33 (3.73)	−0.10 (−0.12)	
B	628.3	3.94	−9.28	
6	587.9 (584.0)	13.2 (20.1)	−19.3 (−33.2)	
7	546.8 (544.2)	2.41 (3.53)	−3.96 (−7.00)	

Further, we deconvoluted the spectra in the Q_y region presuming that there are two $Q_y(0–0)$ bands corresponding to the two $Q_x(0–0)$ bands (the bands 6 and B) because an appearance of one more $Q_y(0–0)$ band was observed by titration with varying amounts of imidazole. The bands 1 and 6 obviously correspond to the $Q_y(0–0)$ and $Q_x(0–0)$ transitions of predominant BChl *a* respectively, therefore, the bands A and B are attributed to $Q_y(0–0)$ and $Q_x(0–0)$ of minor BChl *a* different from one showing the bands 1 and 6. Considering that BChl *a* with the six-coordinated Mg atom in pyridine shows the $Q_x(0–0)$ transitions over 600 nm [5,15], the bands A and B probably originate from the six-coordinated species, and the bands 1 and 6 from the five-coordinated species. We also measured the spectra of BChl *a* in the 3.3 M indole-added CH_2Cl_2. In this case, we were able to decovolute the spectra with the seven components used in hydrophilic solvents (Table 2). Thus, the $Q_x(0–0)$ appeared only at 584 nm, different from that of imidazole. Considering that the CH_2Cl_2 solutions are not acidic, the difference suggests that the interaction of imidazole with the Mg atom seems to be stronger than that of indole because imidazole has a nucleophilic nitrogen in non-acidic solvents to serve as a ligand to Mg whereas indole does not.

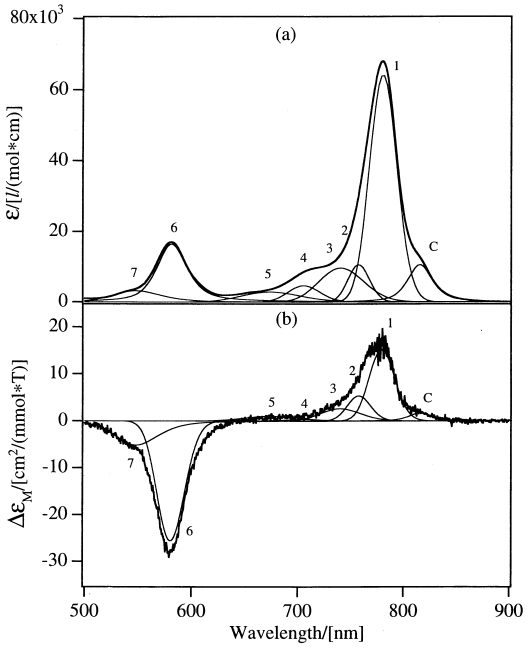

Fig. 5. Deconvolution of the absorption (a) and MCD (b) spectra of BChl *a* in CCl_4. The concentration of BChl *a* was 1.3×10^{-5} mol/l.

Furthermore, the absorption and MCD spectra of BChl *a* in CCl_4 were measured in order to estimate the influence of aggregation on the values of *B*/*D* (Fig. 5). The $Q_y(0–0)$ transition of BChl *a* in CCl_4 appeared at 780 nm and there was another $Q_y(0–0)$ band as a shoulder around 815 nm, which corresponds to aggregated BChl *a*, while the $Q_x(0–0)$ transition is observed only at 580 nm. The MCD intensity of BChl *a* in solvents may be sensitive to a extremely small concentration of polar impurities. However, we found that the impurities do not influence on the aggregation of BChl *a* when BChl *a* is tightly aggregated in CCl_4, because the absorption, CD and MCD spectra were not changed when a very small amount of water or methanol (less than 1 μl; about 3000 times concentration than that of BChl *a*) was titrated in the CCl_4 solution. In the result of deconvolution (Fig. 5), one more component (C) was needed in addition to the seven components used in hydrophilic solvents. The added one component is due to the formation of aggregates of BChl *a* and the band C is considered as the $Q_y(0–0)$ band of the aggregated BChl *a*. The two bands of $Q_y(0–0)$ indicate the existence of two states of BChl *a*, however, the $Q_x(0–0)$ transition could not be deconvoluted to two bands. From this, the BChl *a* molecules absorbing at 780 nm and 810 nm may have the same coordination number.

The results from the deconvolution of the imidazole-, indole-added CH_2Cl_2 and neat CCl_4 solutions, were plotted in Fig. 6 showing a correlation between the *B*/*D* values of $Q_y(0–0)$ and the energy difference of $Q_x(0–0)$ and $Q_y(0–0)$. The positions of BChl *a* in the imidazole-added solution were on the line of monomeric BChl *a* in hydrophilic solvents. The five-coordination state where a imidazole molecule ligates to the Mg atom, locates closely to the position of BChl *a* in dioxane, and the six-coordination state where two imidazole molecules ligate, positioned at upper-right corner. This indicates that imidazole molecules interact strongly with the Mg atom of BChl *a* (see Section 4). The position of the indole-added solution was also on the line and near those of diethyl ether and acetone. Therefore, the interaction of indole molecules with the Mg atoms is similar to those of ether and acetone, that is, weaker than that

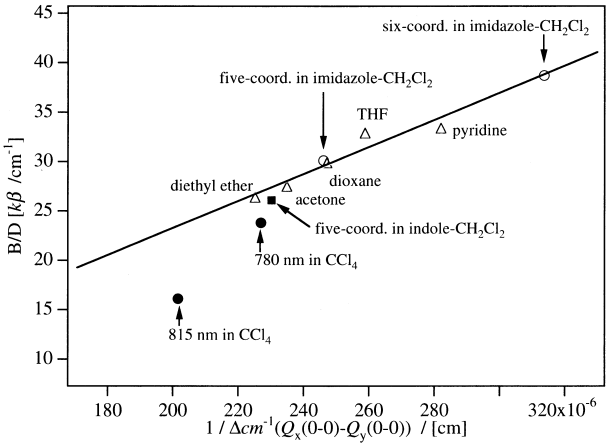

Fig. 6. Correlation between $B/D(Q_y(0–0))$ and $1/\Delta cm^{-1}(6-1)$ for BChl *a* in imidazole-added CH_2Cl_2 solution and CCl_4, where $\Delta cm^{-1}(6-1)$ represents the wavenumber difference between the bands 6 and 1. The solid line is the least squares line for BChl *a* in hydrophilic organic solvents (diethyl ether, acetone, dioxane, THF and pyridine). The data for BChl *a* in imidazole- and indole-added CH_2Cl_2 solution and in CCl_4 were plotted with opened circles, closed squares and closed circles, respectively.

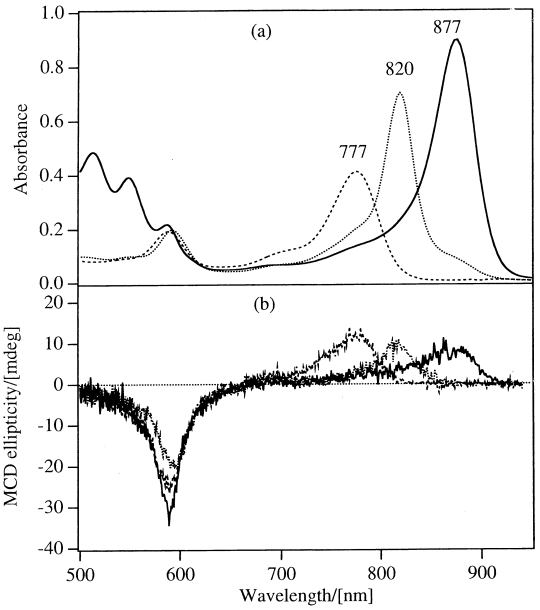

Fig. 7. Absorption (a) and MCD (b) spectra of B777 (dashed line), B820 (dotted line) and B877 (solid line) forms.

of imidazole. In the case of the CCl_4 solution, the two positions were not on the line of monomeric BChl *a*, that is, the *B*/*D* values were smaller than those of monomeric BChl *a* predicted from the energy difference. Considering that BChl *a* tends to aggregate in non-polar solvent [3,50], the interaction between BChl *a* molecules in an aggregate may relate to the decrease of the *B*/*D* values (see Section 4). Thus, the correlation between the *B*/*D* values and the energy difference may be also useful to discuss the formation of aggregates. In this respect, BChl *a* absorbing at 780 nm is very interesting whether it is aggregated or not.

3.3. LH1 treated with β-OG

Fig. 7 shows the absorption and MCD spectra of the LH1 complex at β-OG concentrations of 0.46, 0.75 and 4.0%, and Table 3 lists the wavelengths of absorption maximum of $Q_x(0–0)$ and $Q_y(0–0)$ transitions obtained from deconvolution results. At the β-OG concentration of 0.46%, the $Q_y(0–0)$ transition appeared at 877 nm, while at the 0.75% and 4.0% β-OG the $Q_y(0–0)$ appeared at 820 and 777 nm, respectively (Fig. 7a). The blue-shift reflects the dissociation of the LH1 complex by the increase of β-OG concentration. On the other hand, the $Q_x(0–0)$ transition was shifted very little even at the β-OG concentration of 4.0%, especially in the MCD spectra,

Table 3
The energy difference between the $Q_x(0–0)$ and $Q_y(0–0)$ transitions and the *B*/*D* values of the $Q_y(0–0)$ for the B777, B820 and B877 forms

	$Q_y(0–0)$ (nm)	$Q_x(0–0)$ (nm)	$\Delta cm^{-1}(Q_x-Q_y)$[a] (cm^{-1})	*B*/*D* (kβ/cm^{-1})	predicted *B*/*D*[b] (kβ/cm^{-1})
B777	777	589	4098	29.4	29.3
B820	820	592	4705	22.4	25.1
B877	877	588	5597	9.7	20.5

[a]The $\Delta cm^{-1}(Q_x-Q_y)$ is the difference of wavenumber between the $Q_x(0–0)$ and $Q_y(0–0)$ transitions.
[b]The predicted *B*/*D* was calculated from the value of $\Delta cm^{-1}(Q_x-Q_y)$ as Eq. 2 in the discussion: $B/D=-3.42+1.34\times10^5/\Delta cm^{-1}(Q_x-Q_y)$.

though there is a spectral difference in the 500–600 nm region owing to the removal of carotenoids in the B820 and B777 forms (Table 3 and Fig. 7b). The removal of carotenoids is probably considered to have little effect on the absorption and MCD spectra of BChl *a* since the absorption maximum of Q_y(0–0) in LH1 complexes was only a little blue-shifted (less than 4 nm) and the MCD properties were not changed when the carotenoids in LH1 complexes were removed with the treatment with benzene (data not shown). Therefore, the different changes of Q_y(0–0) and Q_x(0–0) suggest that the Q_x(0–0) transition is less influenced by the formation of aggregates than the Q_y(0–0) transition. Comparison of the absorption and MCD spectra shows that with the dissociation of the LH1 complex the absorbance of the Q_y(0–0) transition decreased while the MCD intensity changed little. This leads to the increase of the *B*/*D* value of Q_y(0–0) transition with the dissociation of the LH1 complex.

When the results of the deconvolution of the LH1 complex were plotted in Fig. 8 showing the correlation between the *B*/*D* values and the energy differences, the B877 form did not fall on the line of monomeric BChl *a*, and the *B*/*D* value was only 47% that for monomer predicted from the energy difference (Table 3). The position of the B820 form

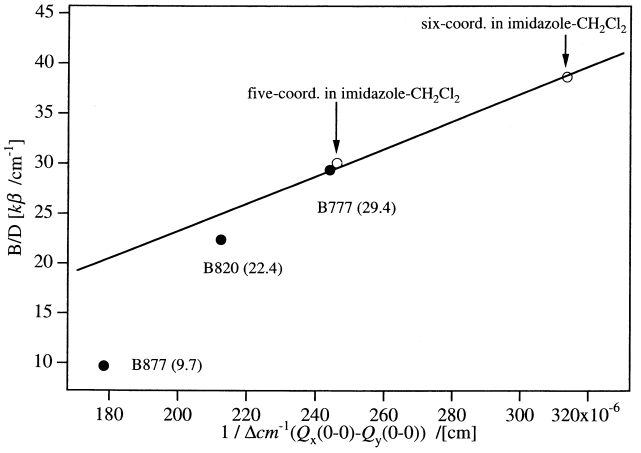

Fig. 8. Correlation between $B/D(Q_y(0–0))$ and $1/\Delta cm^{-1}(6-1)$ for B777, B820 and B877 forms, where $\Delta cm^{-1}(6-1)$ represents the wavenumber difference between the bands 6 and 1 and the data of B777, B820 and B877 forms were plotted with closed circles. The solid line is the least squares line for BChl *a* in hydrophilic organic solvents (diethyl ether, acetone, dioxane, THF and pyridine).

was also not present on the monomeric line, however, the *B*/*D* value (22.4) is closer to the position on the monomeric line than that of the B877 form. The position of the B777 form was present on the line. These facts suggest that the strong pigment-pigment interaction exists in the B877 form and the interaction becomes weaker as the LH1 complex is dissociated. The position of the B777 form was very close to that of the five-coordinated species of BChl *a* in the imidazole-added solution. This indicates that the Mg atom of BChl *a* in the B777 form still has one histidyl residue ligated.

4. Discussion

4.1. Monomeric state

Previously, we reported a correlation of the *B*/*D* value of Q_y(0–0) with the energy difference between Q_x(0–0) and Q_y(0–0) for metal chlorin derivatives [42]. In this study, we found the similar correlation in the metal bacteriochlorin derivative of BChl *a*.

From the theory, the *B*/*D* value of bacteriochlorin derivatives is inversely proportional to the energy difference between the excited states, especially between the closest set of *x*- and *y*- polarized transitions. Therefore, the *B*/*D* value of Q_y(0–0) can be expressed by the following equation [36,42]:

$$\frac{B(Q_y)}{D(Q_y)} = B_0 + \frac{B_1}{E_x - E_y} \quad (1)$$

where E_x and E_y are the energies of the Q_x(0–0) and Q_y(0–0) transitions, respectively, and B_0 and B_1 are constants. The value of B_0 corresponds to the contribution from the excited states other than the excited state of Q_x(0–0), and the value of B_1 corresponds to the mixing between the dipole moments of Q_y(0–0) and Q_x(0–0). In Fig. 3, the least squares line for BChl *a* in hydrophilic organic solvents was as follows:

$$\frac{B(Q_y)}{D(Q_y)} = -3.42 + \frac{1.34\times10^5}{\Delta\,\mathrm{cm}^{-1}} \quad (2)$$

where $\Delta cm^{-1}$is the difference of wavenumber between Q_x(0–0) (band 6) and Q_y(0–0) (band 1). The contribution of B_0 to the *B*/*D* value for BChl *a* in

hydrophilic solvents is much smaller than the second term in Eq. 2 (Fig. 3), suggesting that the B/D value of the $Q_y(0–0)$ is dominated by the mixing with the $Q_x(0–0)$ transition. The B_1 value (1.34×10^5) is slightly small in comparison with that of BChl *c* (1.75×10^5) previously reported, which may indicate that the structural and electronic changes from chlorin to bacteriochlorin influence only a little on the mixing between the dipole moments of $Q_y(0–0)$ and $Q_x(0–0)$.

For metal bacteriochlorin derivatives, a large red-shift of $Q_x(0–0)$ band had been shown to be caused by difference of the solvents used and related to a change from five- to six-coordination state [5]. Furthermore, the absorption maximum of $Q_x(0–0)$ depends not only on the coordination number but also on the nature of the axial ligand [15]. Hartwich et al. [25] pointed out that the red-shift of $Q_x(0–0)$ band is caused by change of the metal coordination. They observed the large shift in the metal bacteriochlorin and the absence of significant shifts in free base bacteriochlorin. The lowest energy $Q_y(0–0)$ transition can be described predominantly as a simple one-electron promotion from HOMO to LUMO, while the second lowest energy $Q_x(0–0)$ transition is a mixture of two one-electron promotions, next HOMO to LUMO, and HOMO to next LUMO [15,36,51]. The effective charge of the central metal atom strongly influences on the next HOMO because of the localization of charge on nitrogen atoms in this orbital. The ligation to the central metal decreases the effective charge of the central metal, which would increase the energy of the next HOMO and cause the red-shift of $Q_x(0–0)$ [15,25]. Therefore, a decrease in the energy difference between $Q_x(0–0)$ and $Q_y(0–0)$ transitions is predominantly attributed to the larger decrease in the transition energy of the $Q_x(0–0)$ by coordination than that of the $Q_y(0–0)$ [7,15].

Fig. 3 shows that even the complexes in the same coordination number have the variation of the energy difference between $Q_x(0–0)$ and $Q_y(0–0)$. This suggests that the effective charge of the metal atom is also changed by the nature of ligand molecules, i.e., the strong interaction of ligand molecules to the Mg atom decreases the energy difference between $Q_x(0–0)$ and $Q_y(0–0)$ by the red-shift of $Q_x(0–0)$. In the case of one imidazole molecule ligating to the Mg, the energy difference is much smaller than those of diethyl ether and acetone (imidazole: 4063 cm^{-1}, diethyl ether: 4441 cm^{-1}, acetone: 4257 cm^{-1}), and the effective charge of the five-coordinated Mg atom seems to be similar to that of the six-coordinated Mg atom with two dioxane molecules. Therefore, these results led to strong interaction of the first coordinating imidazole molecule with the Mg atom. The fact that the metal bacteriochlorin with two imidazole molecules was placed upper-right of that with two pyridine, suggests that the interaction of the two imidazole molecules with the Mg atom is stronger than that of pyridine. The energy difference in the indole-added solution is similar to that of diethyl ether and its location in Fig. 6 is lower than that of the five-coordinated state with one imidazole molecule. Therefore, indole, whose structure is analogous to tryptophan, interacts more weakly with the Mg atom than imidazole.

4.2. In vitro aggregates

BChl *a* is considered to form aggregates in benzene and CCl_4, and several studies have been made to elucidate the aggregated structure and equilibrium between monomer and the aggregates [3,11,22]. Previously, we conducted a small-angle neutron scattering experiment to determine the size of the small aggregates of BChl *a* in benzene [48]. The results indicated that the components absorbing at 781 nm and 817 nm correspond to dimers and a small amount of oligomers, respectively. From the spectroscopic similarity, the BChl *a* in CCl_4 absorbing at 780 nm and 815 nm may correspond to dimers and oligomers, respectively. Fig. 6 shows that the B/D values of the BChl *a* absorbing at 780 nm and 815 nm are smaller than those predicted from the monomeric line. This is apparently attributed to the decrease of the B_1 in Eq. 2, that is, the decrease of the mixing between the dipole moments of $Q_x(0–0)$ and $Q_y(0–0)$. Therefore, the decrease is due to the pigment-pigment interactions caused by aggregation of BChl *a*. The BChl *a* absorbing at 815 nm are more strongly interacting with each other than that absorbing at 780 nm. We previously reported that the B/D value of the special pair of the BChl *a* dimer in the reaction center from *Chromatium tepidum* is about half that for monomeric BChl *a* in diethyl

ether [40], however, the value of the in vitro dimer absorbing at 780 nm was 89% of that predicted from the monomeric line. This difference among the dimers may indicate that the strength of the pigment-pigment interaction depends on the orientation and distance between the BChl *a* molecules in a dimer.

4.3. LH1 complex

The B777 form in Fig. 8 was located on the monomeric line, indicating that there is no pigment-pigment interaction in this form. Sturgis et al. [28] have suggested the conservation of ligation of the histidyl residues in the α or β polypeptides from comparison of absorption and resonance Raman spectra between the B777 form and BChl *a* in an aqueous β-OG solution. Since the position of the B777 form is close to that of BChl *a* ligated by one imidazole molecule, our MCD results may support their suggestion. However, the positions of the B820 and B877 forms were not on the monomeric line, indicating pigment-pigment interaction in both forms. Compared with the difference between the measured *B*/*D* values and those predicted from the monomeric line (Fig. 8 and Table 3), the difference of the B820 form is much smaller than that of the B877 form. Thus, the pigment-pigment interaction probably becomes weak when the B877 form is dissociated to the B820 form. It has been reported that the B877 form is composed of a subunit of B820 form as $\alpha_2\beta_2$BChl$_4$ or $\alpha_3\beta_3$BChl$_6$ [28,46,52], and Visschers et al. [53] reported that the B820 form consists of a strongly interacting dimer of BChl *a* from fluorescence measurements. Our MCD results, however, indicate that the interaction was rather small. The difference in the influence of aggregation between fluorescence and MCD remains uncertain. The B877 form has much stronger pigment-pigment interaction than the B820 form. Comparison to the previous data of the B850 complex in the LH2 and the special pair in the reaction center extracted from *C. tepidum*, shows that the *B*/*D* value of the B877 form was similar to those of the B850 complex (10.6) and the special pair (12.9) [40]. This may indicate that the pigment-pigment interaction is similar between them. Bellacchio et al. [9] noted that the hydrogen-bonding of the C-3 acetyl substituent and C-13 keto group possibly influences the macrocycle energy levels through conjugation with the delocalized π-orbitals, and further, McAuley-Hecht et al. [54] reported that an out-of-plane rotation of the acetyl group affects the absorption properties of $Q_y(0–0)$. We measured the absorption and MCD spectra of BChl *a* in alcohol solvents. The correlation between the *B*/*D* value and the energy difference of $Q_x(0–0)$ and $Q_y(0–0)$ was on the monomeric line of Fig. 3. Hence, we are considering that the value of B_1 in Eq. 1 is little influenced by the hydrogen-bonding of the acetyl and keto groups, especially for chlorin derivatives, we have already reported the independence of the B_1 value from the hydrogen-bonding of the keto group. However for the rotation of the acetyl group, we will have to estimate the effect on the B_1 value. The elucidation for the influence of the acetyl group may lead to a more quantitative analysis of MCD for the LH1 complexes.

In conclusion, we have correlated the *B*/*D* value of Q_y transition with the energy difference between Q_x and Q_y for the pigments with bacteriochlorin backbones. From this correlation, we are able to analyze the ligation state of the Mg atom in BChl *a* and to estimate the influence of pigment-pigment interaction on the mixing between the Q_x and Q_y dipole moments in general. This correlation can be applied to various complexes containing Chl and BChl.

Acknowledgements

We are grateful to Prof. Mamoru Mimuro for discussion. This work was supported by a Grant-in-Aid from the Ministry of Education, Science and Culture, Japan (Nos.: 07750872, 08455377), and JSPS research fellowships for young scientists.

References

[1] J.J. Katz, M.K. Bowan, T.J. Michalski, D.L. Worcester, Chlorophyll aggregation: Chlorophyll/water micelles as models for in vivo long-wavelength chlorophyll, in: H. Scheer (Ed.), Chlorophylls, CRC Press, Boca Raton, FL, 1991, pp. 211–236.

[2] R.E. Blankenship, J.M. Olson, M. Miller, Antenna complexes from green photosynthetic bacteria, in: R.E. Blankenship, M.T. Madigan, C.E. Bauer (Eds.), Anoxygenic Photo-

synthetic Bacteria, Kluwer Academic Publishers, Dordrecht, 1995, pp. 399–435.
[3] K. Sauer, J.R.L. Smith, A.J. Schultz, The dimerization of chlorophyll *a*, chlorophyll *b*, and bacteriochlorophyll in solution, J. Am. Chem. Soc. 88 (1966) 2681–2688.
[4] T.M. Cotton, A.D. Trifunac, K. Ballschmiter, J.J. Katz, State of chlorophyll *a* in vitro and in vivo from electronic transition spectra, and the nature of antenna chlorophyll, Biochim. Biophys. Acta 368 (1974) 181–198.
[5] T.A. Evans, J.J. Katz, Evidence for 5- and 6-coordinated magnesium in bacteriochlorophyll *a* from visible absorption spectroscopy, Biochim. Biophys. Acta 369 (1975) 414–426.
[6] L.L. Shipman, T.M. Cotton, J.R. Norris, J.J. Katz, An analysis of the visible absorption spectrum of chlorophyll *a* monomer, dimer, and oligomers in solution, J. Am. Chem. Soc. 98 (1976) 8222–8230.
[7] K. Sauer, Photosynthetic membranes, Acc. Chem. Res. 11 (1978) 257–264.
[8] L. Limantara, S. Sakamoto, Y. Koyama, H. Nagae, Effects of nonpolar and polar solvents on the Q_x and Q_y energies of bacteriochlorophyll *a* and bacteriopheophytin *a*, Photochem. Photobiol. 65 (1997) 330–337.
[9] E. Bellacchio, K. Sauer, Temperature dependence of optical spectra of bacteriochlorophyll *a* in solution and in low-temperature glasses, J. Phys. Chem. 103 (1999) 2279–2290.
[10] J.J. Katz, G.L. Closs, F.C. Pennington, M.R. Thomas, H.H. Strain, Infrared spectra, molecular weights, and molecular association of chlorophylls *a* and *b*, methyl chlorophyllides, and pheophytins in various solvents, J. Am. Chem. Soc. 85 (1963) 3801–3809.
[11] K. Ballschmiter, J.J. Katz, An infrared study of chlorophyll-chlorophyll and chlorophyll-water interactions, J. Am. Chem. Soc. 91 (1969) 2661–2677.
[12] T.M. Cotton, R.P. van Duyne, Characterization of bacteriochlorophyll interactions in vitro by resonance Raman spectroscopy, J. Am. Chem. Soc. 103 (1981) 6020–6026.
[13] M. Fujiwara, M. Tasumi, Resonance Raman and infrared studies on axial coordination to chlorophylls *a* and *b* in vitro, J. Phys. Chem. 90 (1986) 250–255.
[14] M. Fujiwara, M. Tasumi, Metal-sensitive bands in the Raman and infrared spectra of intact and metal-substituted chlorophyll *a*, J. Phys. Chem. 90 (1986) 5646–5650.
[15] P.M. Callahan, T.M. Cotton, Assignment of bacteriochlorophyll *a* ligation state from absorption and resonance Raman spectra, J. Am. Chem. Soc. 109 (1987) 7001–7007.
[16] G.A. Schick, D.F. Bocian, Resonance Raman studies of hydroporphyrins and chlorophylls, Biochim. Biophys. Acta 895 (1987) 127–154.
[17] G. Hartwich, C. Geskes, H. Scheer, J. Heinze, W. Mäntele, Fourier transform infrared spectroscopy of electrogenerated anions and cations of metal-substituted bacteriochlorophyll *a*, J. Am. Chem. Soc. 117 (1995) 7784–7790.
[18] G.L. Closs, J.J. Katz, F.C. Pennington, M.R. Thomas, H.H. Strain, Nuclear magnetic resonance spectra and molecular association of chlorophylls *a* and *b*, methyl chlorophyllides, pheophytins, and methyl pheophorbides, J. Am. Chem. Soc. 85 (1963) 3809–3821.
[19] J.J. Katz, H.H. Strain, D.L. Leussing, R.C. Dougherty, Chlorophyll-ligand interactions from nuclear magnetic resonance studies, J. Am. Chem. Soc. 90 (1968) 784–791.
[20] S.G. Boxer, G.L. Closs, J.J. Katz, The effect of magnesium coordination on the ^{13}C and ^{15}N magnetic resonance spectra of chlorophyll *a*. The relative energies of nitrogen $n\pi^*$ states as deduced from a complete assignment of chemical shifts, J. Am. Chem. Soc. 96 (1974) 7058–7066.
[21] S. Lötjönen, P.H. Hynninen, Complete assignment of the carbon-13 NMR spectrum of chlorophyll *a*, Org. Magn. Reson. 16 (1981) 304–308.
[22] R.G. Brereton, J.K.M. Sanders, Co-ordination and aggregation of bacteriochlorophyll *a*. An NMR and electronic absorption study, J. Chem. Soc. Perkin Trans. I (1983) 423–430.
[23] R.G. Brereton, J.K.M. Sanders, Bacteriochlorophyll *a*: Assignment of the natural absorbance ^{13}C NMR spectrum. Use fo power spectra, J. Chem. Soc. Perkin Trans. I (1983) 435–437.
[24] P.H. Hynninen, S. Lötjönen, Hydrogen bonding of water to chlorophyll *a* and its derivatives as detected by ^{1}H-NMR spectroscopy, Biochim. Biophys. Acta 1183 (1993) 381–387.
[25] G. Hartwich, L. Fiedor, I. Simonin, E. Cmiel, W. Schäfer, D. Noy, A. Scherz, H. Scheer, Metal-substituted bacteriochlorophylls. 1. Preparation and influence of the metal and coordination on spectra, J. Am. Chem. Soc. 120 (1998) 3675–3683.
[26] M.C. Chang, P.M. Callahan, P.S. Parkes-Loach, T.M. Cotton, P.A. Loach, Spectroscopic characterization of the light-harvesting complex of *Rhodospirillum rubrum* and its structural subunit, Biochemistry 29 (1990) 421–429.
[27] R.W. Visschers, R. van Grondelle, B. Robert, Resonance Raman spectroscopy of the B820 subunit of the core antenna from *Rhodospirillum rubrum* G9, Biochim. Biophys. Acta 1183 (1993) 369–373.
[28] J.N. Sturgis, B. Robert, Thermodynamics of membrane polypeptide oligomerization in light-harvesting complexes and associated structural changes, J. Mol. Biol. 238 (1994) 445–454.
[29] J.D. Olsen, J.N. Sturgis, W.H.J. Westerhuis, G.J.S. Fowler, C.N. Hunter, B. Robert, Site-directed modification of the ligands to the bacteriochlorophylls of the light-harvesting LH1 and LH2 complexes of *Rhodobacter sphaeroides*, Biochemistry 36 (1997) 12625–12632.
[30] B. Robert, M. Lutz, Structure of the primary donor of *Rhodopseudomonas spheroides* difference resonance Raman spectroscopy of reaction centers, Biochemistry 25 (1986) 2303–2309.
[31] M. Lutz and B. Robert, Local enviroments of pigments in reaction centers of photosynthetic bacteria from resonance Raman data, in: M.E. Michel-Beyerle (Ed.), Antennas and Reaction Centers of Photosynthetic Bacteria, Springer-Verlag, Berlin, 1985, pp. 138–146.
[32] R. Gate, A.J. McCaffery, M.D. Rowe, Magnetic circular

dichroism and absorption spectra of the porphyrins. Part I, J. Chem. Soc. Dalton (1972) 596–604.
[33] J.H. Dawson, D.M. Dooly, Magnetic circular dichroism spectroscopy of iron porphyrins and heme proteins, in: A.B.P. Lever and H.B. Gray (Eds.), Iron Porphyrins part 3, VCH publisher, New York, 1989, pp. 1–93.
[34] S. Choi, J.A. Phillips, W. Ware Jr., C. Wittschieben, C.J. Medforth, K.M. Smith, Magnetic circular dichroism spectroscopic studies on the stereochemistry and coordination behavior for nickel porphyrins, Inorg. Chem. 33 (1994) 3873–3876.
[35] C. Houssier, K. Sauer, Circular dichroism and magnetic circular dichroism of the chlorophyll and protochlorophyll pigments, J. Am. Chem. Soc. 92 (1970) 779–791.
[36] J.C. Sutherland, J.M. Olson, Magnetic circular dichroism of bacteriochlorophyll *a* in solution and in a protein, Photochem. Photobiol. 33 (1981) 379–384.
[37] J.D. Keegan, A.M. Stolzenberg, Y.-C. Lu, R.E. Linder, G. Barth, A. Moscowitz, E. Bunnenberg, C. Djerassi, Magnetic circular dichroism studies. 60. Substituent-induced sign variation in the magnetic circular dichroism spectra of reduced porphyrins. 1. Spectra and band assignments, J. Am. Chem. Soc. 104 (1982) 4305–4317.
[38] J.D. Keegan, A.M. Stolzenberg, Y.-C. Lu, R.E. Linder, G. Barth, A. Moscowitz, E. Bunnenberg, C. Djerassi, Magnetic circular dichroism studies. 61. Substituent-induced sign variation in the magnetic circular dichroism spectra of reduced porphyrins. 2. Perturbed molecular orbital analysis, J. Am. Chem. Soc. 104 (1982) 4317–4329.
[39] D. Frackowiak, D. Bauman, H. Manikowski, W. Browett, M. Stillman, Circular dichroism and magnetic circular dichroism spectra of chlorophylls *a* and *b* in nematic liquid crystals II. Magnetic circular dichroism spectra, Biophys. Chem. 28 (1987) 101–114.
[40] M. Kobayashi, Z.-Y. Wang, K. Yoza, M. Umetsu, H. Konami, M. Mimuro, T. Nozawa, Molecular structures and optical properties of aggregated forms of chlorophylls analyzed by means of circular dichroism, Spectrochim. Acta Part A 51 (1996) 585–598.
[41] Y. Nonomura, S. Igarashi, N. Yoshioka, H. Inoue, Spectroscopic properties of chlorophylls and their derivatives. Influence of the molecular structure on the electronic state, Chem. Phys. 220 (1997) 155–166.
[42] M. Umetsu, Z.-Y. Wang, M. Kobayashi, T. Nozawa, Interaction of photosynthetic pigments with various organic solvents. Magnetic circular dichroism approach and application to chlorosomes, Biochim. Biophys. Acta 1410 (1999) 19–31.
[43] L.E. Vickery, T. Nozawa, K. Sauer, Magnetic circular dichroism studies of low-spin cytochromes. Temperature dependence and effects of axial coordination on the spectra of cytochrome *c* and cytochrome b_5, J. Am. Chem. Soc. 98 (1976) 351–357.
[44] J. Michl, Magnetic circular dichroism of cyclic π-electron system. 1. Algebraic solution of the perimeter model for the A and B terms of high symmetry systems with a $(4N+2)$-electron [*n*] annulene perimeter, J. Am. Chem. Soc. 100 (1978) 6801–6811.
[45] J. Michl, Magnetic circular dichroism of cyclic π-electron system. 2. Algebraic solution of the perimeter model for the B terms of systems with a $(4N+2)$-electron [*n*] annulene perimeter, J. Am. Chem. Soc. 100 (1978) 6812–6818.
[46] R. Ghosh, H. Hauser, R. Bachofen, Reversible dissociation of the B873 light-harvesting complex from *Rhodospirillum rubrum* G9+, Biochemistry 27 (1988) 1004–1014.
[47] P.S. Parkes-Loach, J.R. Sprinkle, P.A. Loach, Reconstitution of the B873 light-harvesting complex of *Rhodospirillum rubrum* from separately isolated α- and β-polypeptides and bacteriochlorophyll *a*, Biochemistry 27 (1988) 2718–2727.
[48] Z.-Y. Wang, M. Umetsu, K. Yoza, M. Kobayashi, M. Imai, Y. Matsushita, N. Niimura, T. Nozawa, A small-angle neutron scattering study on the small aggregates of bacteriochlorophylls in solutions, Biochim. Biophys. Acta 1320 (1997) 73–82.
[49] K. Yoza, Z.-Y. Wang, M. Kobayashi, T. Nozawa, High-resolution solid-state ^{13}C NMR of the LH1 from *Rhodospirillum rubrum*, Photosynth. Res. 52 (1997) 167–173.
[50] K. Ballschmiter, K. Truesdell, J.J. Katz, Aggregation of chlorophyll in nonpolar solvents from molecular weight measurements, Biochim. Biophys. Acta 184 (1969) 604–613.
[51] J.D. Petke, G.M. Maggiora, L. Shipman, R.E. Christoffersen, Stereoelectronic properties of photosynthetic and related systems. V. Ab initio configuration interaction calculations on the ground and lower excited singlet and triplet states of ethyl chlorophyllide *a* and ethyl pheophorbide *a*, Photochem. Photobiol. 30 (1979) 203–223.
[52] J.F. Miller, S.B. Hinchigeri, P.S. Parkes-Loach, P.M. Callahan, J.R. Sprinkle, J.R. Riccobono, P.A. Loach, Isolation and characterization of a subunit form of the light-harvesting complex of *Rhodospirillum rubrum*, Biochemistry 26 (1987) 5055–5062.
[53] R.W. Visschers, F. van Mourik, R. Monshouwer, R. van Grondelle, Inhomogeneous spectral broadening of the B820 subunit from LH1, Biochim. Biophys. Acta 1141 (1993) 238–244.
[54] K.E. McAuley-Hecht, P.K. Fyfe, J.P. Ridge, S.M. Prince, C.N. Hunter, N.W. Isaacs, R.J. Cogdell, M.R. Jones, Structural studies of wild-type and mutant reaction centers from an antenna-deficient strain of *Rhodobacter sphaeroides* Monitoring the optical properties of the complex from bacterial cell to crystal, Biochemistry 37 (1998) 4740–4750.